

Interface Strengths in a $\text{ZrO}_2/\text{Ag-Cu-Al-Ti}$ System

Youngmin Lee^a & Jin Yu^b

^aPKG Development, Samsung Electronics Co., Ltd, Seoul, Korea

^bDepartment of Materials Science and Engineering, Korea Advanced Institute of Science and Technology PO Box 201, Chongryang, Seoul, South Korea

(Received 11 November 1994; accepted 28 January 1995)

Abstract: Interface strengths of ceramic/metal joints were investigated using the brazed $\text{ZrO}_2/\text{Ag-Cu-Al-Ti}$ joints prepared under various processing conditions. Interface microstructures and chemistries were investigated using optical microscopy, SEM, X-ray, AES and correlated with flexural strength measurements obtained from the four point bend tests. The amount of segregated S and the thickness of brittle $\text{TiO}/\text{Al}_2\text{O}_3$ layers at the interface were found to be the major factors affecting the interface strength.

1 INTRODUCTION

Brazing of ceramic and metal (C/M) using an active element such as Ti is known to enhance interface strengths by forming interface layers.¹ The interface strength in the C/M joint depends in a very complex way on the residual stress state, interface microstructure, interface chemistry, etc. For example, strengths of the $\text{ZrO}_2/\text{Ag-Cu-Al-Ti}$ joints increased with the formation of $\text{Cu}_3\text{Ti}_3\text{O}$ layer at the C/M interface, but subsequently decreased with the additional formation of TiO .² On the other hand, segregation of S to $\text{Al}_2\text{O}_3/\text{NiCrAl}$ alloy interfaces caused delamination of the ceramic coating.³ In the present work, interfacial microstructure and segregation of residual impurities to C/M interface received particular attention among the many factors which can possibly influence the C/M interface strengths.

2 EXPERIMENTAL PROCEDURE

Zirconia powders stabilized with 3 mol% Y_2O_3 were sintered for 3 h at 1773 K to produce TZP (tetragonal zirconia polycrystals) whose properties are shown in Table 1. The braze alloy with the composition of 51.6 Ag–34.9 Cu–8.7 Al–4.8 Ti (atomic %) was prepared from high purity base

metals by induction melting under 2.7×10^{-1} Pa, and subsequently cold rolled to 150 μm . The amounts of residual S in the braze alloy and base metals are given in Table 2. The filler metals were sandwiched between ZrO_2 pellets and brazed under 2.7×10^{-3} Pa vacuum according to the heat treatment shown in Fig. 1. Three brazing temperatures (1223, 1243 and 1273 K) and three brazing times (0, 20 and 60 minutes) were chosen. Interfacial properties of the C/M joints were examined by scanning electron microscopy (SEM), glancing angle X-ray (with the incident angle of 5°), and Auger electron spectroscopy (AES). Finally, flexural strengths (*FS*) were measured by conducting the four-point bend tests of C/M/C specimens. Experimental details are described extensively in Ref. 4.

3 RESULTS AND DISCUSSION

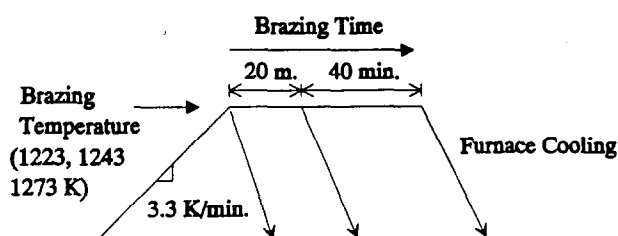
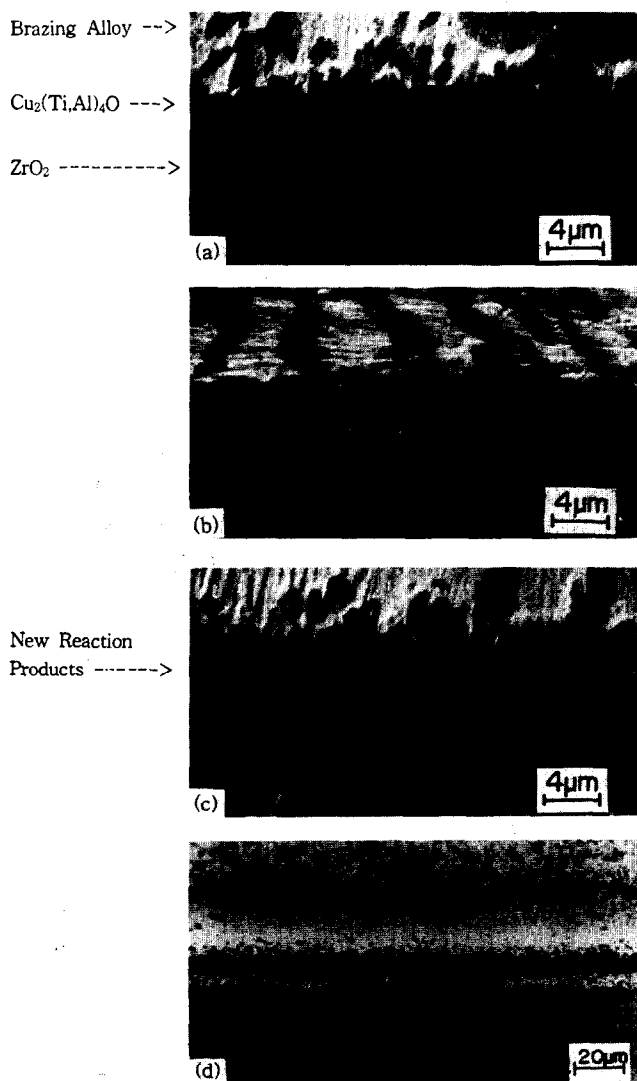
As reported elsewhere,⁵ there are three types of microstructure at the C/M interface, and Fig. 2 shows a typical micrograph of each microstructure. The type 'A' microstructure consists of a $\text{Cu}_2(\text{Ti, Al})_4\text{O}$ layer which is about 0.3–0.4 μm thick and the braze alloy showing off-eutectic microstructure. In the type 'C' microstructure, which was observed at higher brazing temperatures and

Table 1. The characteristics of ZrO_2 used in this experiment

Grain size	Crystal structure	Flexural strength	Fracture toughness
0.45 μm	Tetragonal	$692 \pm 90 \text{ MPa}$	$5.15 \pm 0.12 \text{ MPa m}^{1/2}$

Table 2. The amount of residual S in the braze alloy and base metals used

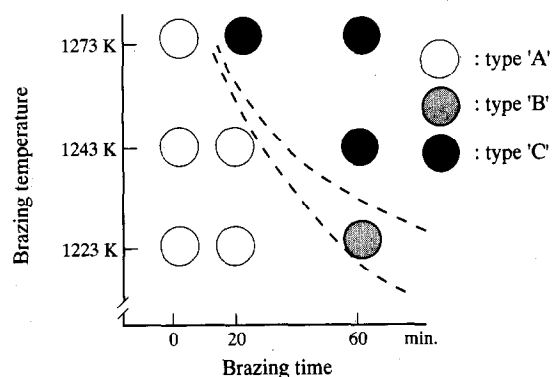
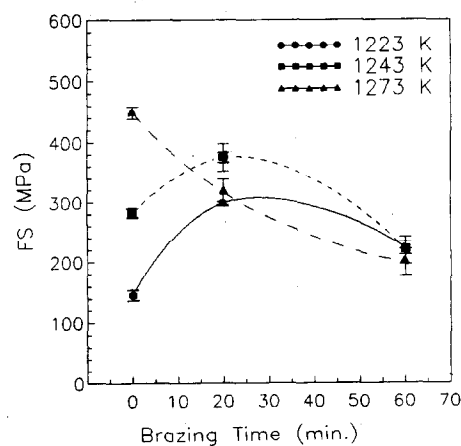
	Braze alloy	Ti	Cu	Al	Ag
S (ppm)	6	13.5	13.3	4.5	4.4

**Fig. 1. Heat treatment cycle used in the brazing process.****Fig. 2. SEM micrographs showing typical (a) 'A', (b) 'B', (c) 'C', and (d) 'C' microstructures. In (d), specimens in (c) were angle lapped and the thickness of the layers appearing in (d) are exaggerated.**

longer brazing times, two new layers identified as $\gamma\text{-TiO}$ and $\alpha\text{-Al}_2\text{O}_3$ were added and the whole structure can be described as $\text{ZrO}_2/\gamma\text{-TiO}/\alpha\text{-Al}_2\text{O}_3/\text{Cu}_2(\text{Ti,Al})_4\text{O}$. The type 'B' microstructure corresponds to a transitional stage between type 'A' and 'C', where discontinuous islands of $\gamma\text{-TiO}/\alpha\text{-Al}_2\text{O}_3$ layers nucleated at the $\text{ZrO}_2/\text{Cu}_2(\text{Ti,Al})_4\text{O}$ interface. Reaction products formed at the C/M interfaces at various processing conditions can be classified into three microstructures and are schematically described in Fig. 3.

In Fig. 4, flexural strengths of C/M/C specimens are shown for the nine brazing conditions. Note that *FS* reaches a maximum at intermediate brazing times at 1223 K and 1243 K, but decreases monotonically with brazing time at 1273 K. Comparisons of *FS* data with the microstructural map of Fig. 3 show that *FS* increases with brazing time and temperature in the region where the type 'A' microstructure dominates but that *FS* decreases with the emergence of the type 'B' or 'C' microstructures.

Examinations of fracture surfaces by SEM and AES did not reveal significant fractographic differences among 'A' specimens but substantial differences in the segregated S content as shown in Figs

**Fig. 3. A schematic diagram showing the type of interface microstructures at various brazing conditions.****Fig. 4. Variations of flexural strength with brazing time at three brazing temperatures.**

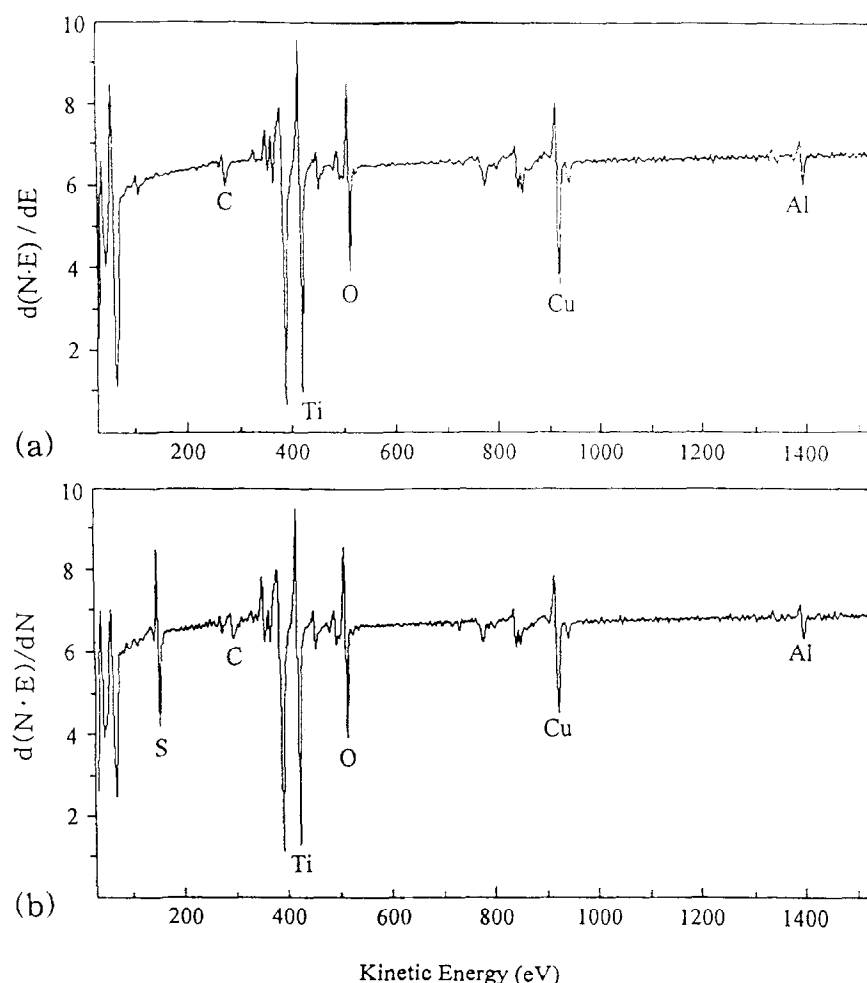


Fig. 5. Auger spectra from fracture surfaces of the 'A' type microstructure from specimens brazed for 0 time at (a) 1273 K and (b) 1223 K.

5 and 6. The S Auger peaks disappeared rapidly with subsequent sputtering which suggested that the S atoms came from the braze alloy and not from the reaction products. Among specimens with the 'A' microstructure, FS decreased with the S content (X_s) on $\text{ZrO}_2/\text{Cu}_2(\text{TiAl})_4\text{O}$ interface as shown in Fig. 6, which is analogous to the grain

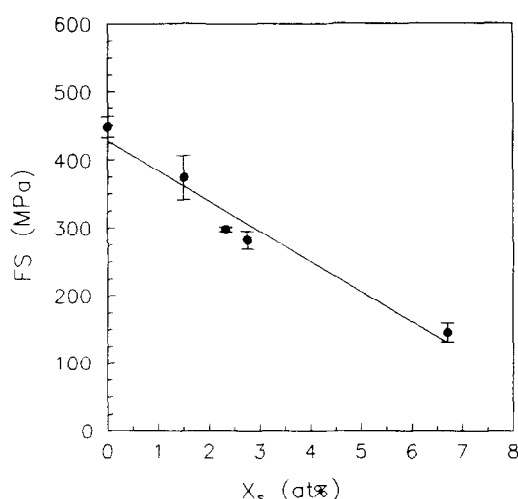


Fig. 6. Variations of the flexural strength as a function of the S content on the fracture surface among the 'A' type specimens.

boundary embrittlement of ferritic steel by residual impurities such as P, Sn, As, Sb and S.⁵

This clearly suggests that the presence of embrittling elements such as S at the C/M interface is a major factor determining the interface strength. It is not clear at the present moment why the S segregation occurs only in the type 'A' microstructures and why it decreases with brazing time. The presence of a brittle phase at the C/M interface is expected to decrease FS , and that was the case for the $\text{TiO}/\text{Al}_2\text{O}_3$ layer at the $\text{ZrO}_2/\text{Cu}_2(\text{Ti,Al})_4\text{O}$ interface. Microhardness measurements of $\text{Cu}_2(\text{Ti,Al})_4\text{O}$, $\text{TiO}/\text{Al}_2\text{O}_3$, and ZrO_2 phases listed in Table 3 show that the $\text{TiO}/\text{Al}_2\text{O}_3$ phase is the hardest of the three. Therefore, the thickness of the $\text{TiO}/\text{Al}_2\text{O}_3$ layer (X_1) at the $\text{ZrO}_2/\text{Cu}_2(\text{Ti,Al})_4\text{O}$ interface was measured for the 'C' type specimens and correlated with FS in Fig. 7. It can be seen that FS decreases with the thickening of the brittle $\text{TiO}/\text{Al}_2\text{O}_3$ layer.

Table 3. Vicker's hardness values of several phases existing near C/M interfaces

$\text{Cu}_2(\text{Ti,Al})_4\text{O}$	$\text{Al}_2\text{O}_3/\text{TiO}$	ZrO_2
1390 ± 168	4559 ± 880	2534 ± 257

So far, we have demonstrated that the two main factors affecting the interface strength are the S content (X_s) and the thickness of the $\text{TiO}/\text{Al}_2\text{O}_3$ layer (X_t) at the $\text{ZrO}_2/\text{Cu}_2(\text{Ti,Al})_4\text{O}$ interface. Are there any other factors with more deleterious effects? We can eliminate the possibility as follows. Firstly, make a hypothesis that FS is a function of X_s and X_t only. Then,

$$FS = f(X_s, X_t) \quad (1)$$

where f is an unknown function.⁶ For small X_s and X_t , we can write

$$FS = f(X_s = 0, X_t = 0) + \left[\frac{\partial f}{\partial X_s} \right]_{X_t} dX_s + \left[\frac{\partial f}{\partial X_t} \right]_{X_s} dX_t \quad (2)$$

ignoring the higher order terms. Secondly, we show that measured FS can be well explained in terms of eqn (2). From Figs 6 and 7, we can rewrite eqn (2) as

$$FS = 443.8 - 44.3 X_s - 222.3 X_t \quad (3)$$

where units of FS , X_s and X_t are given in MPa, atomic %, and μm , respectively. In Fig. 8, FS values calculated from eqn (3) are correlated with experimentally measured FS values, and our hypothesis is justified.

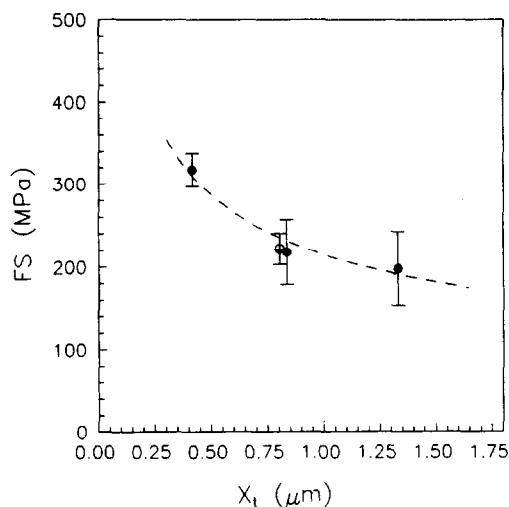


Fig. 7. Variations of the flexural strength as a function of the thickness of $\text{TiO}/\text{Al}_2\text{O}_3$ layer among the 'C' specimens.

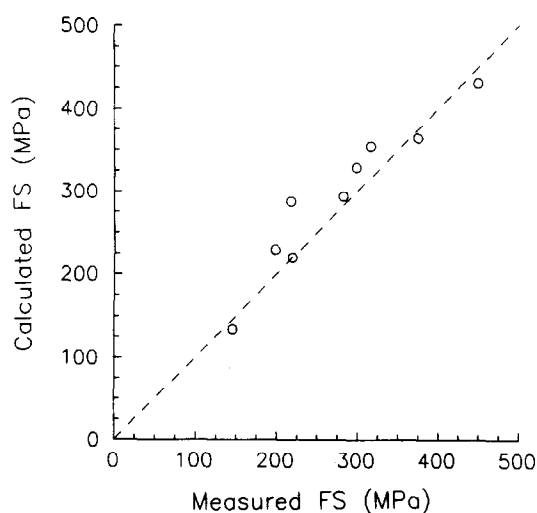


Fig. 8. Comparisons of calculated flexural strength using eqn (3) and experimental data.

4 CONCLUSION

The interface microstructures of $\text{ZrO}_2/\text{Ag-Cu-Al-Ti}$ joints, are basically $\text{ZrO}_2/\text{Cu}_2(\text{Ti,Al})_4\text{O}$ or $\text{ZrO}_2/\gamma\text{-TiO}/\alpha\text{-Al}_2\text{O}_3/\text{Cu}_2(\text{Ti,Al})_4\text{O}$ types which depend sensitively on the brazing temperature and time. Two main factors detrimental to the interface strength are the amount of S segregation at the C/M interface and the thickness of the $\text{TiO}/\text{Al}_2\text{O}_3$ layer. Thermodynamics of the S segregation are not clear at the present moment.

REFERENCES

1. LOEHMAN, R. E. & TOMSIA, A. P., *Amer. Ceram. Soc., Bull.*, **67**(2) (1988) 375.
2. ISHIKAWA, T., BIRTO, M. E., INOUE, Y., HIROTSU, Y. & MIYAMOTO, A., *ISIJ International*, **30** (1990) 1071.
3. FUNKENBUSCH, A. W., SMEGGIL, J. G. & BORNSTEIN, N. S., *Metall. Trans. A.*, **16** (1985) 1164.
4. LEE, Y. M. & YU, J., *Scripta Met. et Mat.*, **29** (1993) 371.
5. MCMAHON, C. J. Jr. & MARCHUT, L., *J. Vac. Sci. Tech.*, **15** (1978) 450.
6. RICE, J. R. & J. S. WANG, *Mat. Sci. Eng.*, **A107** (1989) 23.